On the Role of Biophysical Properties of Cortical Neurons in Binding and Segmentation of Visual Scenes

Paul F. M. J. Verschure
Institute of Neuroinformatics, ETH-UZ, 8057 Zürich, Switzerland; Salk Institute, La Jolla, CA 92037, U.S.A., and Neurosciences Institute, San Diego, CA 92121, U.S.A.

Peter König
Institute of Neuroinformatics, ETH-UZ, 8057 Zürich, Switzerland, and Neurosciences Institute, San Diego, CA 92121, U.S.A.

Neuroscience is progressing vigorously, and knowledge at different levels of description is rapidly accumulating. To establish relationships between results found at these different levels is one of the central challenges. In this simulation study, we demonstrate how microscopic cellular properties, taking the example of the action of modulatory substances onto the membrane leakage current, can provide the basis for the perceptual functions reflected in the macroscopic behavior of a cortical network. In the first part, the action of the modulatory system on cortical dynamics is investigated. First, it is demonstrated that the inclusion of these biophysical properties in a model of the primary visual cortex leads to the dynamic formation of synchronously active neuronal assemblies reflecting a context-dependent binding and segmentation of image components. Second, it is shown that the differential regulation of the leakage current can be used to bias the interactions of multiple cortical modules. This allows the flexible use of different feature domains for scene segmentation. Third, we demonstrate how, within the proposed architecture, the mapping of a moving stimulus onto the spatial dimension of the network results in an increased speed of synchronization. In the second part, we demonstrate how the differential regulation of neuromodulatory activity can be achieved in a self-consistent system. Three different mechanisms are described and investigated. This study thus demonstrates how a modulatory system, affecting the biophysical properties of single cells, can be used to achieve context-dependent processing at the system level.

1 Introduction

Elucidating the relation of results found at different levels of description is one of the central challenges of the neurosciences, which spans subdisciplines ranging from molecular biology to ethology. The problem is aggravated by the fact that no single level provides complete information.

Theoretical studies are therefore useful to investigate the implications of assumptions made in the description of the system at each level and especially to use the description available at other levels for cross validation (Verschure, 1998).

Using a simulation of primary visual cortex, we demonstrate that the biophysical properties of cortical neurons can play a decisive role in the binding and segmentation of visual stimuli. Basic properties of neurons, described by the membrane time constant and electrotonic length constant, are determined by the capacitance and conductance of the membrane (Rall, 1969, 1977; Connors, Gutnick, & Prince, 1982; McCormick, Connors, Lighthall, & Prince, 1985; cf. Llinas, 1988; Amitai & Connors, 1995; Yuste & Tank, 1996). These constants (e.g., the membrane conductance) are not fixed, but can be influenced by a multitude of factors. First, the potassium leakage current is a major constituent of the membrane conductivity and can be affected by neuromodulatory substances such as acetylcholine (ACh) acting via the muscarinic receptor (the I_m current) (McCormick, 1992; Wang & McCormick, 1993; Wilson, 1995; cf. McCormick, 1993). Second, synaptic input itself can increase the membrane conductance and thus increase the total electrotonic length of a dendrite (Bernander, Douglas, Martin, & Koch, 1991). Third, active conductances can have a profound influence on the properties of dendritic signal transduction, which, however, can no longer be described by Rall's classical equations (Softky, 1994). Thus, dynamic dendritic properties, which influence the propagation of any postsynaptic potential toward the soma, can play a pivotal role in signal integration.

Within the context of a neuronal circuit, these microscopic biophysical properties can have pronounced effects on the spatiotemporal interactions of neurons, in particular on the synchronization and desynchronization of neuronal activity. These macroscopic phenomena are a focus of current research. Experimental evidence shows that in the mammalian cerebral cortex, synchronization of neuronal activity reflects Gestalt laws of grouping individual components of the visual scene into objects (Singer & Gray, 1995; König & Engel, 1995). These observations support earlier hypotheses that these phenomena are the basis of binding and segmentation of visual scenes (Milner, 1974; von der Malsburg, 1981; Shimizu, Yamaguchi, Tsuda, & Yano, 1986). Individual objects are represented by assemblies of neurons firing synchronously. Different objects, in turn, are represented by distinguished neuronal assemblies, whose activities have no systematic temporal relationship.

Experimental evidence shows that the synchronization of neuronal activity is mediated by tangential connections in the cortex (Engel, König, Kreiter, & Singer, 1991; Löwel & Singer, 1992; König, Engel, Löwel, & Singer, 1993; Nowak, Munk, Nelson, James, & Bullier, 1995). These connections effectively implement the Gestalt laws describing image segmentation (Koffka, 1922; Köhler, 1930). Their effectiveness, however, is influenced by the dendritic integration of the postsynaptic potentials. In particular, se-

lecting different subsets of afferent synapses by changing the electrotonic properties of the dendritic tree leads to changes in the effective connectivity and spatiotemporal interactions in the neuronal circuit.

Here we demonstrate, first, that the spatial scale of synchronization and desynchronization can be modulated to achieve context-dependent binding and segmentation of input stimuli. Second, we show that the strength of modulatory input, acting on the leakage current, can be used to bias the interactions of multiple cortical modules. This facilitates the flexible use of different feature domains for scene segmentation. Third, we demonstrate how, within the proposed architecture, the movement of a visual stimulus over time is mapped onto the spatial dimension of the neuronal network, resulting in a near-instantaneous binding. Fourth, three different mechanisms for closed-loop control of the level of ACh release are described and results reported.

Thus, this study relates several effects on the macroscopic scale to their underlying microscopic mechanisms. It demonstrates how a modulatory system acting on the biophysical properties of single cells can adapt the system to the global properties of input stimuli leading to their context-dependent processing. Parts of the results have been published previously in abstract form (König & Verschure, 1995).

2 Methods and Results

In this study the interaction of large numbers of model neurons is investigated under a variety of stimulus conditions. The system incorporates excitatory, inhibitory, and modulatory connections. The modeled interactions were chosen to reflect the action of several neurotransmitters and receptor types; glutamic acid and the AMPA (α-amino-3-hydroxy-5-methyl-4-isoxazole propionic acid) receptor, GABA (γ-aminobutyric acid) and the GABA A and GABA B receptors, and ACh and the muscarinic receptor. As a naming convention the simulated populations of cells will be identified in terms of the transmitter or receptor they employ in signaling. We present the equations governing the dynamics of the individual units, followed by the description of the connectivity of the full network.

2.1 Neuronal Model. The behavior of a neuron is modeled through state variables describing the dynamics of the underlying currents, receptors, and channels. The leaky integrate-and-fire unit will generate a spike when its membrane potential exceeds its spiking threshold. The activity of unit i at time t, $S_i(t)$, is given by:

$$S_i(t) = H(V_i(t) - \theta), \tag{2.1}$$

where H is the Heaviside function, $V_i(t)$ represents the membrane potential of cell i at time t, and θ is the firing threshold. Thus, $S_i(t)$ is a binary vari-

Table 1: Properties of the Modeled Cell Populations.

Name	Size	θ	ϵ	A^c	β
Glutamate	400	0.99	0.75	2	2
GABA A	400	0.40	0.75	1	0.70
GABA B	100	0.50	0.80	–	0.05

Note: Size gives the number of units used in each module of the simulation. θ is the firing threshold; ϵ determines the decay constant of the membrane potential; A^c is the default attenuation of the dendrite; β represents the strength of the afterhyperpolarization after a spike is generated.

able indicating the presence or absence of an action potential at time t. In case an action potential is generated, the membrane potential V_i is reset by subtracting a fixed hyperpolarization value β (see Table 1).

The membrane potential of cell i, V_i, is determined by the integrated synaptic input and the passive decay toward the resting potential of 0. The excitatory and inhibitory input to cell i are integrated at the soma according to

$$V_i(t+1) = \epsilon\, V_i(t) + \sum_{j=1}^{N_i} S_j(t - \tau_{ij})\, W_{ij}\, e^{-A_i(t)D_{ij}}. \qquad (2.2)$$

ϵ determines the speed of the passive decay of the membrane potential and as such reflects the integration time constant. Subscripts j and i refer to the pre- and postsynaptic units, respectively; N_i is the total number of excitatory and inhibitory inputs to unit i. The polarization at the soma due to the input is determined by the integral over the time-delayed, τ, afferent activity, S, weighted by the respective synaptic efficacy, W, and attenuated according to the distance of the synapse to the soma, D, and the log-attenuation factor, A, of the dendrite.

The modulatory input has no direct influence on the membrane potential, but affects the dendritic integration of excitatory and inhibitory signals. The dendrite of each unit is modeled as an equivalent cylinder as given by Rall (1969). The attenuation of postsynaptic potentials propagating toward the soma is characterized by the log-attenuation factor $A_i(t)$ (Zador, Agmon-Snir, & Segev, 1995) and the distance of the synapse from the soma D_{ij}. The electrotonic length of neuron i, and thus the attenuation of postsynaptic potentials, A_i, is influenced by the modulatory afferents:

$$A_i(t) = A^c - \sum_{j=1}^{M_i} S_j(t - \tau_{ij})\, W_{ij}. \qquad (2.3)$$
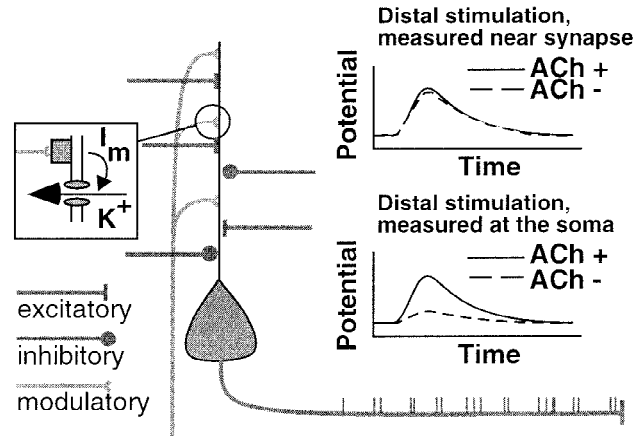
Figure 1: A simplified scheme of the effects of ACh on the propagation of synaptic potentials. Excitatory and inhibitory synapses are placed at varying distances from the soma. The modulatory system is assumed to act via the muscarinic receptor and the I_m current, reducing an outward potassium current, K^+ (box). The local depolarization due to the stimulation of a distal synapse is not affected by the activity of the modulatory system (upper panel). However, it influences the attenuation of a postsynaptic potential toward the soma. If the modulatory system is not active, the effective contribution of a distal postsynaptic potential to the membrane potential as measured at the soma will be strongly attenuated (lower panel, dashed line). In contrast, if the modulatory units are highly active, the neuron is electrotonically compact, and the postsynaptic potentials of the distal and proximal parts of the dendritic tree are conducted to the soma with little attenuation (lower panel, solid line). The spike train plotted on the axon (duration approximately 300 ms) is representative of the activity of a simulated excitatory neuron.

where A^c is the baseline value of the attenuation, and M_i denotes the number of modulatory inputs. The value $A_i(t)$ determines the set of effective synapses and thus which part of the afferent input is integrated (see Figure 1).

In the simulated unit, the effect of an afferent action potential is independent of the current value of the membrane potential. In real neurons, however, the presynaptic transmitter release acts on the membrane conductance by opening or closing synaptic channels. The synaptic current and the change in membrane potential it induces, in turn, depend on the current value of the membrane potential. This effect can lead to a saturation of the dendritic membrane potential and sublinear summation of postsynaptic potentials (Mel, 1994). This mechanism is employed in our investigation of the closed-loop control of ACh release described in section 2.7. In gen-

eral, however, the inclusion of voltage-dependent channels may cancel or even reverse this effect (Softky, 1994). Furthermore, because the somatic membrane potential, the variable modeled here, has an upper limit at the threshold for the generation of action potentials below the reversal potential of the mixed currents due to excitatory input, the effect of postsynaptic saturation of excitatory postsynaptic potentials is limited. The reversal potential of inhibitory currents, in contrast, is in the range of the resting membrane potential or slightly lower. This opens the possibility that inhibition acts in a multiplicative fashion and not in a subtractive one, as assumed here. Nevertheless, detailed simulations have shown that in active neurons of this type, inhibition is effectively subtractive (Holt & Koch, 1997). In summary, given the level of detail of this simulation, the assumption that the postsynaptic effect of afferent action potentials is independent of the current value of the membrane potential seems to be a reasonable and useful approximation.

2.2 The Module. Systems consisting of one or more modules are investigated. Each module consists of five different populations of units: excitatory, fast and slow inhibitory, modulatory, and input (see Table 1 and Figure 2). One of the five maps, Input, is used to supply sensory input to the excitatory units of population Glutamate. Because the actual generation of feature selectivity is not within the scope of this article and is investigated elsewhere (Ferster & Koch, 1987; Douglas, Koch, Mahowald, Martin, & Suarez, 1995; Somers, Nelson, & Sur, 1995), the input was preprocessed to reflect the distribution of local features in the visual scene. In the simulations described below each population is mapped onto an idealized cross-section through an ice cube model (Hubel & Wiesel, 1998). Thus, one axis of the two-dimensional map represents different values of the feature, while the other axis corresponds to the spatial position of the receptive field. These afferents, however, constitute only a small part of the total number of synapses within the module. The actual responses of the units can be, and are, affected by the internal connectivity, which consists of local inhibitory and long-range excitatory interconnections. Both types of inhibitory units project to a local neighborhood of topographically corresponding excitatory units. Excitatory projections to both types of inhibitory populations, in turn, contact a local neighborhood of topographically corresponding units. Excitatory projections within population Glutamate have a wide arborization.

A central feature of the model is the placement of connections on the dendritic tree. The distance of synapses originating and terminating in populations Glutamate or GABA A is dependent on the distance between presynaptic and postsynaptic neurons (see Table 2). Synapses connecting nearby neurons—those with similar receptive fields and feature selectivities—are placed relatively proximal. Connections between neurons farther apart, i.e., with dissimilar receptive fields and/or feature selectivities, are placed progressively more distal on the dendritic tree. Postsynaptic potentials from

cell populations

Input

Glutamate

GABA A

GABA B

ACh

feature

←— **space** —→
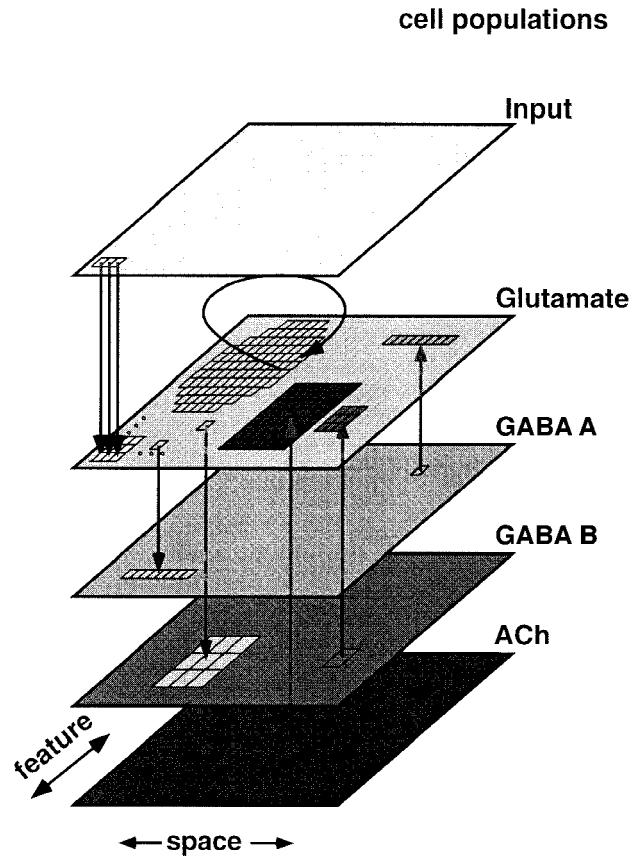
Figure 2: Simulated module. Each module consists of five populations of units represented as inclined squares: input, glutamate, GABA A, GABA B, ACh. Each population is arranged in a two-dimensional map with topographic connections within and between maps. The quantitative parameters of all connections are given in Table 2.

these synapses are subject to a varying amount of attenuation depending on the state of the modulatory system. This arrangement allows the translation of different sets of effective synapses, selected by the modulatory system, into variations of the range of tangential coupling.

Within a network with a fixed anatomy, a change in the electrotonic properties of excitatory and inhibitory units leads to a change in the effective connectivity between those units. Depending on the values of D_{ij}, $A^{Glutamate}$, and $A^{GABA\ A}$ these arrangements can be characterized by four major types of interactions:

Table 2: Properties Synapse Types Used.

Efferent Population	Afferent Population	Size	Arborization (Width:height)	W Range (Min:max)	τ (Offset:Δ)	D (Offset:Δ)
Input	Glutamate	400	1:1	1.0:1.0	0:0	0:0
*Glutamate	Glutamate	59136	15:15	0.0:0.2	0:1	1:1
*Glutamate	GABA A	2560	1:7	0.45:0.45	1:1	0:1
Glutamate	GABA B	841	3:3	0.1:0.1	1:0	0:0
*GABA A	Glutamate	2560	1:7	-0.225:-0.675	1:1	0:0.5
GABA B	Glutamate	3136	3:3	-2.25:-2.25	0:0	0:0
ACh	Glutamate	400	1:1	4.0:4.0	0:0	0:0
ACh	GABA A	400	1:1	4.0:4.0	0:0	0:0

Note: The parameters defining connections marked with * are initialized dependent on the distance between connected cells. In this case the actual strength of a synapse, W_{ij}, is defined by $min + d_{ij}^n(max - min)$, where d_{ij}^n represents the distance between cells i and j normalized for the maximum distance possible given the arborization width and height. The transmission delay, τ_{ij}, and the distance of synapse j, D_{ij}, are defined by Offset $+ d_{ij}\Delta$. In this case d_{ij} is defined as the Cartesian distance between cells i and j.

1, when $A^{Glutamate}$ and $A^{GABA\ A}$ remain at their initial values of 2 and 1 respectively, the interactions within population Glutamate and between Glutamate and GABA A will be restricted. Thus, most of the postsynaptic potentials onto a cell will be strongly attenuated. This mode of interaction will be referred to as "uncoupled." In this case, the activity of cells in population Glutamate will be dominated by the excitatory postsynaptic potentials generated by activity in population Input.

2, when a small modulatory input to populations Glutamate and GABA A is provided, nearest neighbors can interact. This condition is referred to as "local."

3, at a medium range of modulatory input, $A^{GABA\ A}$ will approach 0 while $A^{Glutamate}$ will approximate 1. In this case, all postsynaptic potentials onto cells in population GABA A will be effective; also, the inhibitory postsynaptic potentials onto Glutamate will barely be affected by dendritic attenuation. However, the excitatory postsynaptic potentials generated in population Glutamate, due to interactions within this population will still be affected by $A^{Glutamate}$. The behavior of cells in Glutamate will now be dominated by both the excitatory postsynaptic potentials generated by population Input, the inhibitory postsynaptic potentials generated by cells in population GABA A, and to a limited extent by the lateral interactions within population Glutamate. This condition will be referred to as "column."

4, with a further increase of the modulatory input, the cells in population Glutamate will become fully compact. In this case, all excitatory postsynaptic potentials generated by interactions within population Glutamate will

contribute to the depolarization of these cells. In this condition, referred to as "global," the firing of cells in Glutamate will reflect the contribution of population Input, the inhibition received from population GABA A, and the excitatory postsynaptic potentials generated by interactions within population Glutamate.

2.3 Data Analysis and Simulation Environment. The interaction between different units has been investigated with cross-correlation analysis. The count of spikes of two units occurring at a particular time lag was normalized with the geometric mean of the total number of spikes of the respective units. This normalization makes the resulting cross-correlogram independent of the level of activity and allows the computation of measures like contribution, efficiency, effect on activity, and effect on timing (Levick, Cleland, & Dubin, 1972; Neven & Aertsen, 1992; König, Engel, & Singer, 1995).

Simulations were performed using the environment IQR421, developed by Verschure (1997). It supports a graphical programming language, based on X-Motif, to define large-scale heterogeneous neural systems. It includes tools for real-time presentation of stimuli and the analysis of the dynamics of the network. Furthermore, it allows continuous logging of all variables, analysis, and documentation.

The simulation environment has been developed using C for a UNIX environment. Computations can be performed in a distributed fashion using the TCP/IP protocol. Our simulations were performed on a SUN Ultra 1 and a cluster of PentiumPro PCs.

2.4 Context-Sensitive Segmentation. In accounts of binding by synchronization, it is assumed that neurons representing features (e.g., orientation, disparity, or color) relating to the same object in the visual scene are synchronized. However, what is considered similar is not a static property, but a function of the overall context. For a visual scene with nearly constant hue, minor variations in color can lead to a segmentation of figure from background. If the range of colors represented is large, minor variations in color are not that salient and will not affect segmentation (Nothdurft, 1994). Such a flexible range of segmentation is difficult to achieve in a network with fixed connectivity.

Here, context-sensitive segmentation was investigated using visual scenes containing different ranges of color values (see Figure 3). The first case considered consists of colored rectangles with small local variations in color but large global variation (see Figure 3A). The Gestalt laws of perception would predict that this scene should be segmented into two groups consisting of the four left and the four right rectangles. For the second case, the local variability of the color of the rectangles is identical to the previous one (see Figure 3B). However, the global range of colors represented is reduced. Thus, the visual scene should be segmented into an interdigitating pattern

of four units, each representing identical colors, irrespective of their spatial distance.

This task requires different spatial scales of interactions in the network, which is achieved by the modulatory system coupled to the total electrotonic length of the simulated cortical neurons. In this section we focus on the effect of one element of the whole loop, the action of the modulatory system on the effective neuronal interactions in the cortical network. Hence, we are using an externally set level of ACh activity. For the visual scene containing a large range of color values, it is chosen to operate in condition column. This leads to a strong coupling of units representing identical and similar colors (see Figure 3A, dashed and solid lines). Units representing very different colors show no consistent phase relationship (dotted line). Thus, this visual scene is segmented into two components, consisting of the four patches to the left and the four patches to the right.

In contrast, for the second stimulus (see Figure 3B) the global range of colors represented is reduced. Thus, the network is operated under condition local. This leads to a synchronization of units representing identical colors, irrespective of their spatial distance (dashed and dotted lines). Units representing similar but not identical color values, however, are not synchronized (solid line). Thus, a segmentation into two interdigitated groups of four patches is observed.

In both experiments, the left part of the visual scene is identical. However, the active units are either grouped together or segmented into an interdigitated pattern, expressing global properties of the visual scene. This context-sensitive segmentation is determined by the activity of the modulatory system. Thus, the modulatory system can tune the effective coupling within the network to fit the global properties of the input stimulus and in this way affect the segmentation constructed by the network.

2.5 Interfeature Domain Segmentation and Binding. An important property of the visual system is the flexibility with which different feature domains can interact to achieve binding and segmentation of visual stimuli. In a real-world scene, for instance, disparity is an important cue for scene segmentation. Even in the absence of all other cues, as in a random dot stereogram, segmentation based solely on disparity is possible. However, when a scene is presented as a two-dimensional photograph, the identical disparity across the image should create a strong, misleading cue. Nevertheless, segmenting visual stimuli presented as photographs usually does not pose any particular problems to human observers.

In this experiment, a visual scene is investigated that contains segmentation cues in one feature domain only. The network consists of three modules, each identical to the one described before, representing orientation, disparity, and color, respectively (see Figure 4). The connections between the modules are reciprocal and similar to the long-range projections within a module and are implemented by projections between the excitatory maps.
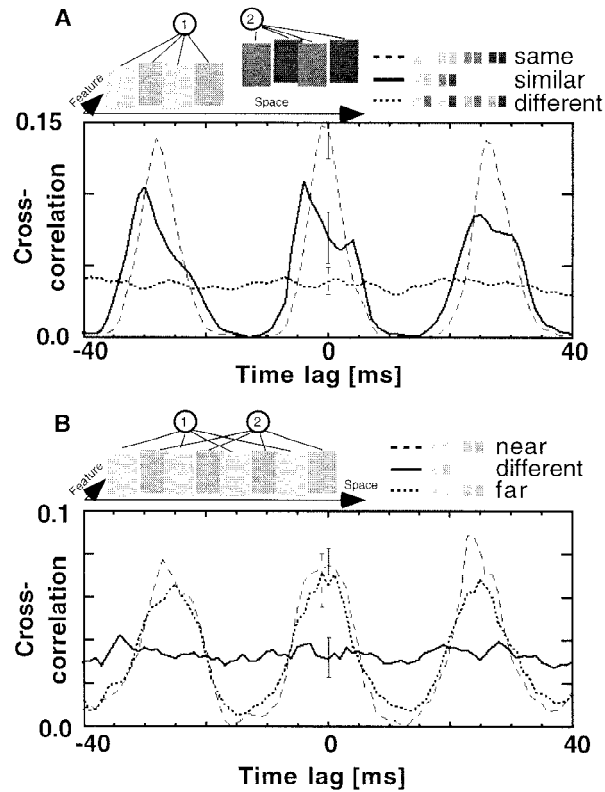
Figure 3: Single module context-sensitive segmentation. (A) The top part shows the mapping of the visual scene onto the two-dimensional network. Different colors in the stimulus are represented using a gray scale. The lower panel shows the normalized cross-correlation functions for all pairs representing identical colors (indicated in gray scale, dashed lines), similar colors (solid lines), and dissimilar colors (dotted lines). The error bars give the standard deviation of the cross-correlation at zero time lag over the respective set of pairs of neurons. The numbers in circles indicate the segmentation of the visual scene generated by the module into two components. (B) The second stimulus used (top) has a smaller variability in the color domain. The correlation patterns (bottom) for pairs of units representing identical colors either neighboring (dashed line) or distant (dotted line) or similar colors (solid line) are shown. The error bar for the pairs of neurons with similar feature preferences but far apart (dotted line) has been shifted to the left for clarity. All data have been averaged across 10 trials.
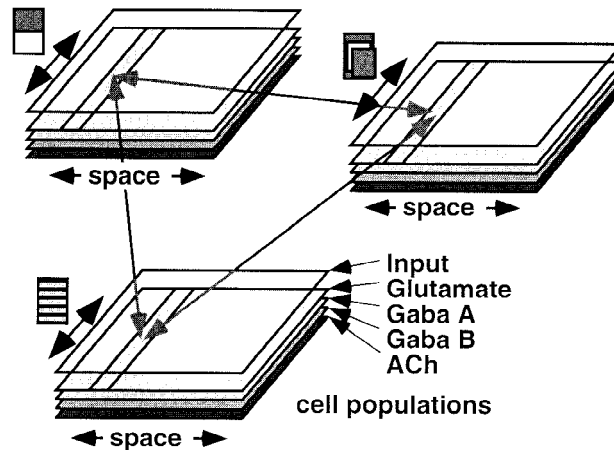
Figure 4: Connectivity of the multiple module system. Each module consists of five classes of units represented by the stacks of squares as shown in Figure 2. In each module, one dimension represents space, and the second dimension represents either color, disparity, or orientation, as indicated by the icons to the left of the respective stack. Connectivity between modules is solely defined by excitatory connections. These connections cover the complete feature dimension in the target module but are restricted in the spatial dimension.

The connectivity between modules was restricted to spatially overlapping receptive field positions, but not restricted in the feature dimension. Furthermore, the connections between different modules are symmetric, each module projecting to the other two in the described fashion. The modulatory system projects independently to all three modules. This implies a topographic specificity of these projections. The topographic organization of basal forebrain projections has been studied in many different species, and an ordered projection has consistently been found (Ruggiero, Giuliano, Anwar, Stornetta, & Reis, 1990; Baskerville, Chang, & Herron, 1993). Furthermore, the size of an individual cholinergic axonal arbor is rather limited. Thus, any inhomogeneity of the activity level in the basal forebrain nuclei results in an inhomogeneous cholinergic innervation of the cortical network similar to the one assumed in the model presented here.

The dynamics of neuronal interactions within and between the three modules was investigated with stimuli that generated different activity patterns in the three modules. The color module was stimulated with a pattern similar to the one used in Figure 3B. This module is operated in condition column and is referred to as the dominant module. The two other modules received a homogeneous input pattern. Because the variability of the stimulus in these two modules is low, they are operated in condition local, and,
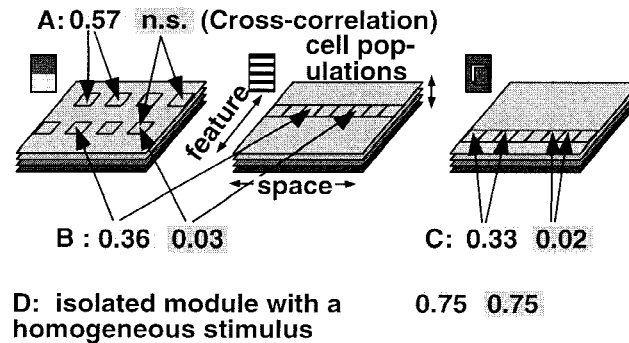
Figure 5: Dynamics in the multiple module system. The three modules representing color, orientation and disparity, as indicated by the icons, are represented by stacks of four squares each. For clarity, population Input has been omitted. Optimally stimulated units are shown as inclined squares. The averaged cross-correlation coefficient at zero-phase lag of neuronal activity is shown for several classes of pairs: (A) units representing identical colors and units representing different colors in the dominant module, (B) units representing the same spatial location in different modules and units representing spatial neighboring but not identical locations in different modules, and (C) units of the nondominant orientation or disparity modules, where the matching locations in the color module received identical stimuli and units representing orientation and disparity where units in the color module at matching locations received different stimuli. The color module was operated in condition column, the two other modules in condition local. (D) The average cross-correlation of units in isolated modules with homogeneous stimuli operated in condition local.

they are referred to as the nondominant modules. This input configuration reflects the properties of a visual scene that contains only segmentation cues in one of several feature domains.

In Figure 5 the resulting pattern of zero-phase-lag correlations is shown. The cross-correlation at zero time lag between units representing identical colors is high (A: 0.57); the cross-correlation of units representing different colors, however, is not significantly different from zero (A: n.s.). Thus, the stimulus is segmented correctly in the color module, although it is coupled to two other modules receiving homogeneous stimuli. Furthermore, this synchronization pattern is imposed onto the two other modules. Units in different modules representing identical spatial positions are strongly correlated (B: 0.36), irrespective of the associated feature values, while those at neighboring positions do not show any coupling (B: 0.03). This demonstrates a segmentation of the stimulus in the nondominant orientation and disparity modules following the dominant color module. This is further exemplified by the coupling shown of units representing the respective fea-

tures at locations corresponding to bound units in the color module (C: 0.33), irrespective of their spatial distance. In contrast, units representing orientation and disparity values at locations where the color in the dominant module is not identical are not correlated (C: 0.02). This difference is even more remarkable because this case includes pairs of directly neighboring units.

In a control simulation of isolated modules, operated in condition local, as the nondominant modules above, a homogeneous stimulation leads to a strong correlation of all active units (D: 0.75). This demonstrates that the segmentation derived in the nondominant modules is induced by the dominant module. However, this does not imply that the intermodule connections lead to a transfer of feature selectivity. In fact, because the connections between modules are not feature specific, units in the orientation and disparity module cannot be selective with respect to color.

In summary, the input stimulus is segmented into two assemblies, each spanning all three modules. Each assembly comprises units representing identical color in one module and all active units in the other modules at corresponding spatial locations. The active units in the two nondominant modules are segmented into an interdigitated pattern as determined by the dominant module. Thus, by including the dynamic regulation of dendritic integration, the interaction between different cortical modules can be balanced to reflect the relative contribution of individual feature domains to the segmentation task at hand.

2.6 Binding of Moving Stimuli. In many physiological experiments dealing with the fast dynamics of neuronal activity, simple moving geometric patterns are used as visual stimuli, since these stimuli effectively activate cortical neurons. Due to the movement of the stimulus, the activated region is moving through the cortex. This implies that the interactions among units separated in space, mediated by the tangential connections, are now mapped onto interactions in time. Therefore, the behavior of the model was investigated under these conditions.

The dynamics of synchronization were compared between a smoothly moving and a static rectangle. The activity and cross-correlation of six immediately neighboring units along the spatial axis was monitored. Figure 6 shows the comparison between the two stimulus conditions for both the onset and steady-state response.

In the case of a moving stimulus, both the steady-state and the response onset cross-correlation show the same degree of synchronization (see Figure 6A). In contrast, the first spikes elicited by the static stimulus are not synchronous (see Figure 6B).

The enhanced coherence in the response to moving stimuli can be explained by the induction of subthreshold oscillations in the membrane potential of cells neighboring the active units. Thus, compared to static stimuli, this leads to a faster synchronization. In fact, the first spike, triggered by the
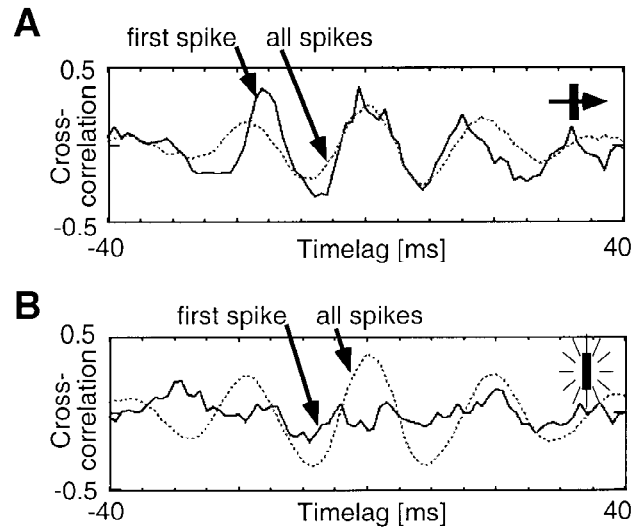
Figure 6: Binding moving stimuli. (A) Cross-correlation functions of unit activity for the moving stimulus, averaged over all combinations of cell pairs, taking into account the first spike of each unit only (solid line) and all spikes (dashed line). Note that the synchronization of the first spike is approximately as strong as the average over all spikes. (B) Cross-correlation functions obtained using a static stimulus. Note that the first spikes are not synchronized in this condition. Data were gathered over 10 trials, and the network was operated in condition column.

appearance of the stimulus in the receptive field of a unit, was already synchronous (see Figure 6A).

2.7 Closing the Loop. In the simulations described above, the activity of the modulatory system is set as an external parameter. For a self-contained system like the real brain, however, it needs to be a function of the system's own activity. An important element of such a self-contained regulatory system should be that its complexity is lower than that of the main processing circuitry itself. Given this constraint, a self-contained regulatory system can be defined in several ways.

First, statistical information on the input pattern can be used. Measures like the total activity level and the variance of features present in the stimulus can be defined using highly convergent connections and does not require detailed global information. In this case, a single readout unit receives convergent connections from all units in population Glutamate of one module. Here we exploit the fact that afferents targeting the same dendritic segments may lead to saturation of the postsynaptic potential and thus to a sublinear

increase of the induced synaptic currents (Mel, 1994). Maintaining the topographic relationship of the projecting neurons in the placement of synapses on the dendritic tree allows the postsynaptic unit to measure the variability of the feature distribution in the projecting population. The readout unit, in turn, forms excitatory projections on the respective ACh units, thus forming a positive feedback loop. It regulates the activity of ACh and the resulting dendritic attenuation in populations Glutamate and GABA A with the variability of the feature distribution of the represented stimuli. Because the activity in the sending module builds up very quickly, the time constant of this type of feedback loop can be very short. In our simulations a steady-state level of ACh was reached after about 10 ms. We tested this mechanism with the input stimuli shown in Figures 3A and B and the input pattern of the nondominant modules shown in Figure 5. These patterns are examples of activity distributions, which have high, medium, and low feature variability. Using these stimuli, the positive feedback induces a level of ACh activity of 0.78, 0.41, and 0.16 respectively. This compares well with the values used in the open-loop simulation above (0.8, 0.4 and 0.2). Because the closed loop leads to a nontrivial dynamics of the ACh level, the segmentation of the stimulus shown in Figure 3B was further analyzed. Similar to the results shown in Figure 3B, units representing identical colors were significantly correlated (0.09), while the correlation of those units representing different colors was not significantly modulated. Thus, this simple and straightforward mechanism exploits statistical properties of the input stimulus to produce a rough estimate of the appropriate ACh level very quickly, leading to a context-sensitive segmentation using positive feedback and the distribution of features in the stimulus while ignoring spatial and temporal properties.

An alternative method is to measure the level of synchronization in a module and use it to down-regulate the level of ACh. To explore this negative feedback circuit, a readout unit was defined that acts as a coincidence detector and receives input from all excitatory units in a module. This unit in turn inhibits the respective ACh units. In the case of global synchrony in the projecting population, the input to this unit is phase locked and reaches high levels. This implements a negative feedback loop relating the level of synchrony within a module to the ACh influence on it. The dynamics of this type of closed loop is somewhat slower because some time is needed to "measure" the degree of synchrony. In our simulations the characteristic timescale was of the range of 100–200 ms (no attempt was made to probe the lower limit). We tested this mechanism with the input stimulus shown in Figure 7A. The ACh level starts out high, at a maximum of 0.97, and is then subject to the dynamics of the closed loop as soon as the stimulus appears. Initially global synchronization is observed, involving pairs representing identical colors (see Figure 7B) as well as pairs representing different colors (see Figure 7C). Within a few hundred milliseconds the ACh level reaches the range of 0.6 to 0.7, where it stabilizes (average of 0.63). By this time, the
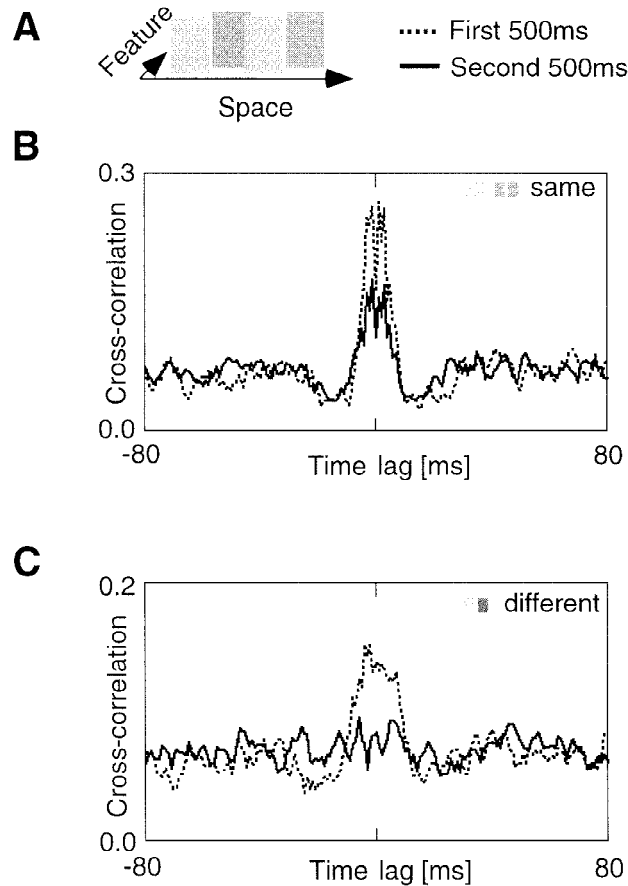
Figure 7: A self-regulatory system. (A) Stimulus used for the investigation of a regulatory mechanism based on the readout of the level of synchrony in a module. Cross-correlation functions of units representing (B) identical features or (C) different features. The dotted lines give the cross-correlation functions averaged over the first 500 ms after stimulus presentation. The solid lines show the correlation during the interval from 500 ms to 1000 ms after stimulus presentation. At 500 ms, the ACh activity had already reached a steady-state level roughly equivalent to condition column.

correlation of those units representing different features is desynchronized, and those representing identical features are still synchronized. Thus the synchronization pattern observed is qualitatively similar to the simulation described above (see Figure 3B) where a fixed level of ACh activity was used. This mechanism exploits the statistical properties of the temporal dy-

namics within a module to form a negative feedback loop but ignores spatial and feature information.

The formation of a synchronization pattern in a module is not the last step in the processing of sensory events; it needs to be read out by other areas. In these areas, neurons might have more complex receptive fields and invariance properties. This allows a third type of closed loop to be defined. The activity level in a module on a higher level of the hierarchy establishes the negative feedback loop that inhibits the ACh activity at the preceding level. This ensures the formation of synchronization patterns that have some interpretation within the framework of the processing hierarchy. This mechanism can be seen as complementary to lateral inhibition. As opposed to reducing weakly activated representations, it sorts out the input pattern and reduces cross-talk in those situations by allowing a favorable segmentation to arise. The modulatory control exploits the complexity of the cortical network itself and can be kept surprisingly simple. This type of closed-loop regulatory system is subject to current investigation. Preliminary results show that it is the most robust mechanism, but also the slowest of those considered (Verschure & König, unpublished data).

In summary, all three methods seem to be workable solutions to close the loop between the modulatory system and the dynamics of neuronal activity within a module. The first two mechanisms exploit statistical properties of the activity pattern, one concentrating on the feature distribution, the other on temporal properties. Therefore, the circuit of the closed regulatory loop can be kept simple. The third mechanism relies on the complexity of the cortical network. Therefore, all three regulatory mechanisms are much simpler than the system they regulate. Furthermore, their properties are complementary, the fastest mechanism providing a rough estimate only and the most sophisticated mechanism being the slowest, while contributing high-level information. Thus, a combination of all three mechanisms seems to be the most viable approach.

3 Discussion

The task of scene segmentation has been addressed in many simulations (von der Malsburg, 1995). In these studies, temporal coding has been used for binding sets of active neurons into coherent assemblies. In most cases, however, a fixed effective anatomy was used. Therefore, due to the pre-specified interactions, only limited sets of stimuli could be successfully segmented. The model presented here addresses several problems that arise in these fixed architectures and links the dynamic scaling of cortical interactions to a modulatory system acting on the biophysical properties of neurons. First, it establishes a mechanism for regulating the degree of coherence and the segmentation of sensory input on different spatial scales. The implemented system reflects some properties of the cholinergic system of the basal forebrain. Second, the interaction of several modules containing

independent cues for scene segmentation was studied. In a previous investigation (Schillen & König, 1994), a system with fixed effective interaction was proposed. This system, however, was limited to stimuli suitable for the spatial scale of the implemented interaction, and the scene was segmented according to a majority vote of all modules. In our investigation, the modulatory system allows emphasizing the modules containing segmentation cues. In this way a flexible contribution of each module to scene segmentation is achieved, which scales favorably with an increasing number of modules. Third, the segmentation of moving stimuli was explored. The tangential interactions in the neuronal network not only lead to a synchronization of active neurons, but also speed up binding of assemblies of neurons that are just becoming activated by the moving stimulus by inducing subthreshold oscillations in the membrane potential of neighboring cells. This will bias the timing of the response of the cell once a stimulus appears in its receptive field. Thus, the proposed dynamic regulation of dendritic integration by a modulatory system seems to be important for the development of a system that can flexibly adapt to a wide range of stimuli. Fourth, multiple ways were investigated of closing the loop between the modulatory system and the activity of units in a module. The loop can be closed using both a positive and a negative feedback loop. In all cases, the circuitry of the regulatory loop is of a much lower complexity than the connectivity of the simulated cortical module. Remarkably, it is possible to tap into the machinery made available by the hierarchy of modules in a sensory system to define a sophisticated control using a simple circuit.

3.1 Assumptions and Predictions of the Model.

3.1.1 Finite Electrotonic Length of Cortical Neurons. In the presented model, we made the assumption that the attenuation of postsynaptic potentials varies in a range equivalent to a total electrotonic length of the neuron between 0 and 4. Available studies using intracellular recording techniques give values in the range of 1 to 2 (Bindman, Meyer, & Prince, 1988). These studies are supported by estimates of the electrotonic structure of cortical neurons based on anatomical data (Tsai, Carneval, Claiborne, & Brown, 1994). However, several recent studies indicate that the electrotonic length of cortical neurons might be larger. First, experiments using the patch clamp technique seem to indicate a higher internal resistance of the core conductor (Spruston, Jaffer, Williams, & Johnston, 1993), which would increase the estimates of the electrotonic length by a factor of 2 to 4. Second, background activity can increase the membrane conductance and thus increase attenuation of signals propagating in the dendrite considerably (Bernander et al., 1991). Third, the electrotonic structure of a neuron as seen from the soma is often compact. However, as seen from a synapse placed on the dendritic tree, the electrotonic structure of a pyramidal neuron often resembles the anatomical structure, that is, sites on the distal apical dendritic tree are electrotonically

quite remote (Zador et al., 1995). Fourth, the measurements cited above refer to the attenuation of steady-state signals. However, the attenuation of transient signals, which are the important events in the present context, is stronger (Rall, 1977; Agmon-Snir & Segev, 1993). Thus, measurements of the electrotonic length of cortical neurons using steady-state signals underestimate the true attenuation. Taken together, these studies indicate that the electrotonic structure of cortical neurons leaves a large dynamic range for the modulation of signals from the apical dendritic tree and that a value for the electrotonic length in the range of 0 to 4 is a reasonable choice.

3.1.2 Spatial Distribution of Synapses.   In our model we assume that the distribution of synapses on the dendritic tree is dependent on the similarity of receptive field properties of the pre- and postsynaptic neurons. Due to the topographic order in the cortex, this implies a dependence on the physical distance as well. This assumption is supported by physiological and anatomical studies. Current source density measurements have shown that after an electric shock to the optic chiasm, activity flows sequentially from layer 4 to lower layer 3 and from there to long-distance connections terminating in layer 2 (Mitzdorf & Singer, 1978). These delays increase for sites located closer to the cortical surface. This study also showed that the synapses between distant neurons are formed in the distal dendritic tree. Furthermore, anatomical studies indicate that the position of synapses on the dendritic tree is an increasing function of the distance between the soma of the pre- and postsynaptic neurons (Thomson & Deuchars, 1994). Thus, several lines of research indicate that the placement of synapses on the dendritic tree of cortical neurons is not random. Actually, we view the proposition made here of a monotone relationship between the similarity of receptive field properties of two connected neurons and the electrotonic distance from the soma of the respective synapse as a particularly simple example of a specific wiring and expect that combined anatomical and physiological studies will uncover more specific and complex properties of synaptic placement on the dendritic tree in the future.

3.1.3 The Interactions Between Binding and a Modulatory System.   The model presented in this article goes beyond available experimental data in several respects. First, the basic effect of context-sensitive synchronization can be deduced from the published hypothesis of binding by synchronization. Yet stimuli of this complexity have not been used extensively in physiological experiments. Therefore, we propose not only a concrete mechanism that can explain such a performance, but also predict that the suppression of the modulatory system or manipulation of its site of action should interfere with the binding and segmentation of such stimuli. Second, our modeling study suggests that the dynamic balancing of modules processing different feature domains is critically dependent on the modulatory system. Thus, maintaining high activity of the modulatory system in those modules that

receive homogeneous stimuli should lead to a change of the synchronization pattern in the module that receives structured input, that is, to global synchronization similar to the isolated module with homogeneous stimulation. A test of these two predictions seems to be within the reach of existing experimental techniques.

3.1.4 Simplifications Made.   Even in a model of considerable complexity, many simplifications have to be made. Although this work investigates the relation of a particular biophysical mechanism with macroscopic properties, no attempt was made to use a biologically realistic model neuron. Thus, many known properties—and, of course, all the unknown as well—have been ignored—most notably, the active properties of dendrites. In recent years many interesting results on voltage gated channels and active propagation of action potentials in dendrites have been found. The effect of voltage-dependent channels is of particular interest since they may boost weak currents (Ca^{++} channels) or attenuate them (K^+ channels). The precise interaction between modulatory system and these channels depends on the sequence of their actions. If, for example, similar to the effect of dopamine in neurons in prefrontal cortex (Seamans, Gorelova, & Yang, 1997), these channels are located in the proximal dendrite, it acts like a threshold, increasing the differential effect of the modulatory system. Voltage-dependent potassium channels counteract this effect and introduce a temporal component to these interactions. Depending on the precise density and location of these channels, many different scenarios are possible. However, given the current state of research, a very large number of parameters are not known. It could be argued that including voltage -dependent channels with slower kinetics interferes with the proposed mechanism. For instance, the NMDA channel is best known for its role as a sort of coincidence detector. For its activation, it needs not only the binding of transmitter molecules but also a postsynaptic depolarization to release the Mg^{++} block. Although transmitter binding is a slow process, the release of the Mg^{++} block is fast, and thus the resulting postsynaptic current has a fast dynamics. Due to the attenuation of postsynaptic potentials, this mechanism would be dependent on the spatial specificity of synaptic placement. Although its role in changing synaptic efficacy is well studied, many questions regarding its distribution and the function under in vivo conditions are currently not resolved. In summary, to investigate the effects of active dendritic processes seems to be a promising field of research; however, including a myriad of unknown parameters in a modeling study could easily obscure its results.

More directly related to the model presented here are other sources affecting membrane properties that have been neglected. This applies to the increased membrane conductance due to synaptic input as well as the effect of voltage-dependent channels. The properties of these two mechanisms are partly similar and partly complementary. For example, a stimulus with a small variation in feature properties (like the one shown in Figure 3, lower

panel) leads to a larger input via the tangential connections than a stimulus comprising widely different feature values (like the one shown in Figure 3, upper panel). Thus, the increased input would lead to a stronger increase in membrane conductance, similar to the effect of the modulatory system in that simulation. On the other hand, changes in the strength of the afferent input interfere with this mechanism, but not necessarily with a modulatory system, as described in this study. Similar arguments can be made for the effect of, for instance, voltage-dependent potassium channels. For this reason we decided to demonstrate the feasibility of dynamic modulation of neuronal interactions in a minimal system. To combine these different mechanisms in a single model to increase the biological realism as well as its performance will be an interesting future study.

3.2 Modulatory Systems. In biological systems many different forms of modulation are known (Katz & Frost, 1996). Here we call an effect modulatory if it does not by itself activate or inhibit a neuron. Furthermore, the action of a modulatory system is typically not on a fast timescale. It can be thought of as setting the appropriate working range for the fast dynamics on a timescale of a few dozen milliseconds. This study involves an external set of neurons that influence the properties of dendritic integration of neurons in a whole area and do not have receptive fields comparable to cortical neurons. These properties are inspired by the nucleus basalis magnocellularis (NBM) of Meynert, the main source of cholinergic projections to the cerebral cortex. This region has been shown to contain a large number of cells responsive to visual stimuli (Santos-Benitez, Magarinos-Ascone, & Garcia-Austt, 1995). The arborization patterns of the cholinergic projections arising in this region, and terminating in the cerebral cortex, have shown to be topographically specific (Baskerville, et al., 1993). The termination pattern of these subcortical projections is mainly on dendritic shafts. These modulatory systems in general affect the excitability of the target neurons and influence their signal-to-noise ratio (Foote & Morrison, 1987). A possible sensory interface for this region can be found in the amygdala, which receives abundant cortical and subcortical inputs conveying sensory events and projects to the NBM. Hence, our model study proposes that areas such as NBM play a more active role in sensory processing than traditionally believed.

In this study, the effect of ACh on the K^+ current was considered, through which dendritic integration in cortical neurons can be regulated. In particular, closing channels that support a leak current leads to a decrease of the membrane conductivity and thereby to a more efficient transmission of postsynaptic potentials from the distal dendritic tree to the soma. The position of the muscarinic receptors at the dendritic shafts of cortical cells puts them in a prime location to control the dendritic integration of the postsynaptic potentials generated by cortico-cortical interactions. Actually, recent studies found an influence of the activation of the parabrachial nucleus on

the synchronization of cortical neurons (Munk, Roelfsema, König, Engel, & Singer, 1996). Furthermore, Steriade, Dossi, Pare, & Oakson (1991) show an enhancement of gamma band activity by stimulation of the mesopontine cholinergic nuclei. Thus, the modulatory system as used in the simulation resembles the properties of the cholinergic system.

4 Conclusions

In this article we explored the relationship between the biophysical properties of cortical neurons and their collective dynamics at the system level. In particular, we proposed that a modulatory system, acting on the membrane leakage current of cortical neurons, influences the electrotonic length and thus the properties of dendritic integration. We demonstrated that such a mechanism can support the segmentation and binding of visual stimuli at varying spatial and temporal scales. To evaluate the performance of the proposed model, we described four experiments. The first demonstrated that by regulation of the dendritic space constant, input stimuli could be segmented on a varying spatial scale dependent on the stimulus context. The second set of experiments investigated the interaction of different feature domains in a system consisting of multiple modules. We showed that by a differential regulation of the dendritic space constant, a segmentation derived in one feature domain could be superimposed onto other feature domains. The third experiment showed the effect of the modulatory system onto the dynamics of binding moving stimuli. It demonstrated that by enhancing the excitability in cortical circuits, the coherence of a bound subassembly could be preserved while it moved through the map. In the last set of simulations, we considered three different methods to relate the ACh activity to the dynamics in the processing modules. The feasibility of a closed regulatory loop was demonstrated and some of the complementary properties of the different methods explored. In conclusion, this study establishes that the microscopic biophysical properties of cortical cells can play a decisive role in the perceptual functions reflected in the macroscopic properties of cortical circuits.

Acknowledgments

References

Agmon-Snir, H., & Segev, I. (1993). Signal delay and input synchronization in passive dendritic structures. *J. Neurophysiol., 70*, 2066–2085.

Amitai, Y., & Connors, B. W. (1995). Intrinsic physiology and morphology of single neurons in neocortex. In E. G. Jones, I. T. Diamond, (Eds.), *Cerebral cortex, 11* (pp. 299–301). New York: Plenum Press.

Baskerville, K. A., Chang, H. T., & Herron, P. (1993). Topography of cholinergic afferents from the nucleus basalis of Meynert to representational areas of sensorimotor cortices in the rat. *J. Comp. Neuro., 335*, 552–562.

Bernander, O., Douglas, R. J., Martin, K. A. C., & Koch, C. (1991). Synaptic background activity influences spatiotemporal integration in single pyramidal cells. *Proc. Natl. Acad. Sci. USA, 88*, 1569–1573.

Bindman, L. J., Meyer, T., & Prince, C. A. (1988). Comparison of electrical properties of neocortical neurones in slices in vitro and in the anaesthetized rat. *Exp. Brain Res., 69*, 489–496.

Connors, B. W., Gutnick, M. J., & Prince, D. A. (1982). Electrophysiological properties of neocortical neurons in vitro. *J. Neurophysiol., 48*, 1302–1320.

Douglas, R. J., Koch, C., Mahowald, M., Martin, K. A.C., & Suarez, H. H. (1995). Recurrent excitation in neocortical circuits. *Science, 269*, 981–985.

Engel, A. K., König, P., Kreiter, A. K., & Singer, W. (1991). Interhemispheric synchronization of oscillatory neuronal responses in cat visual cortex. *Science, 252*, 1177–1179.

Ferster, D., & Koch, C. (1987). Neuronal connections underlying orientation selectivity in cat visual cortex. *Trends Neurosci., 10*, 487–492.

Foote, S. L., & Morrison, J. H. (1987). Extrathalamic modulation of cortical function. *Ann. Rev. Neurosci., 10*, 67–95.

Holt, G. R., & Koch, C. (1997). Shunting inhibition does not have a divisive effect on firing rates. *Neural Comput., 9*, 1001–1013 .

Hubel, D. H., & Wiesel, T. N. (1998). Early exploration of the visual cortex. *Neuron, 20*(3), 401–412.

Katz, P. S., & Frost, W. N. (1996). Intrinsic neuromodulation: Altering neuronal circuits from within. *Trends Neurosci., 19*:55–61.

Koffka, K. (1922). Perception: An introduction to the Gestalt theory. *Psychological Bulletin 19*, 531–585.

Köhler, W. (1930). *Gestalt psychology*, London : Bell and Sons.

König, P., & Engel, A. K. (1995). Correlated firing in sensorimotor systems. *Current Opinion in Neurobiology, 5*, 511–519.

König, P., Engel, A. K., Löwel, S., & Singer, W. (1993). Squint affects synchronization of oscillatory responses in cat visual cortex. *Eur. J. Neurosci., 5*, 501–508.

König, P., Engel, A. K., & Singer, W. (1995). Relation between oscillatory activity and long-range synchronization in cat visual cortex. *Proc. Nat. Acad. Sci. USA, 92*, 290–294.

König, P., & Verschure, P. F. M. J. (1995). Subcortical control of the synchronization of cortical activity: A model. *Soc. Neurosci. Abstr. 21*.

Levick, W. R., Cleland, B. G., & Dubin, M. W. (1972). Lateral geniculate neurons of cat: Retinal inputs and physiology. *Invest. Ophthalmol. Vis. Sci., 11*, 302–311.

Llinas, R. R. (1988). The intrinsic electrophysiological properties of mammalian neurons: Insights into central nervous system function. *Science, 242*, 1654–1664.

Löwel S., & Singer, W. (1992). Selection of intrinsic horizontal connections in the visual-cortex by correlated neuronal-activity. *Science, 255*, 209–212.

McCormick, D. A. (1992). Cellular mechanisms underlying cholinergic and noradrenergic modulation of neuronal firing mode in the cat and guinea pig dorsal lateral geniculate nucleus. *J. Neurosci., 12*, 278–289.

McCormick, D. A. (1993). Actions of acetylcholine in the cerebral cortex and thalamus and implications for function. *Prog. Brain Res., 98*, 303–308.

McCormick, D. A., Connors, B. W., Lighthall, J. W., & Prince, D. A. (1985). Comparative electrophysiology of pyramidal and sparsely spiny stellate neurons of the neocortex. *J. Neurophysiol., 54*, 782–806.

Mel, B. (1994). Information processing in dendritic trees. *Neural Comp., 6*, 1031–1085.

Milner, P. M. (1974). A model for visual shape recognition. *Psychol. Rev., 81*, 521–535.

Mitzdorf, U., & Singer, W. (1978). Prominent excitatory pathways in the cat visual cortex (A 17 and A 18): A current source density analysis of electrically evoked potentials. *Exp. Brain Res., 33*, 371–394.

Munk, M. H. J., Roelfsema, P. R., König, P., Engel, A. K., & Singer, W. (1996). Role of reticular activation in the modulation of intracortical synchronization. *Science, 272*, 271–274.

Neven, H., & Aertsen, A. M. H. J. (1992). Rate coherence and event coherence in the visual-cortex—A neuronal model of object recognition. *Biol. Cybern., 67*, 309–322.

Nothdurft, H. C. (1994). Common properties of visual segmentation. *Ciba Found. Symp., 184*, 245–259.

Nowak, L. G., Munk, M. H. J., Nelson, J. I., James, A. C., & Bullier, J. (1995). Structural basis of cortical synchronization, 1. Three types of interhemispheric coupling. *J. Neurophysiol., 74*, 2379–2400.

Rall, W. (1969). Time constants and electrotonic length of membrane cylinders and neurons. *Biophys J., 9*, 1483–1508.

Rall, W. (1977). Core conductor theory and cable properties of neurons. In E. R. Kandel (Ed.), *Handbook of physiology* (pp. 39–97). Bethesda, MD: American Physiological Society.

Ruggiero, D. A., Giuliano, R., Anwar, M., Stornetta, R., & Reis, D. J. (1990). Anatomical substrates of cholinergic-autonomic regulation in the rat. *J. Comp. Neuro., 292*, 1–53.

Santos-Benitez, H., Magarinos-Ascone, C. M., & Garcia-Austt, E. (1995) Nucleus basalis of Meynert cell responses in awake monkeys. *Brain Res. Bull., 37*, 507–511.

Schillen, T. B., & König, P. (1994). Binding by temporal structure in multiple feature domains. *Biol. Cybern., 45*, 106–155.

Seamans, J. K., Gorelova, N. A., & Yang, C. R. (1997). Contributions of voltage-gated Ca2+ channels in the proximal versus distal dendrites to synaptic integration in prefrontal cortical neurons. *J. Neurosci., 17*, 5936–5948.

Shimizu, H., Yamaguchi, Y., Tsuda, I., & Yano, M. (1986). Pattern recognition based on holonic information dynamics: towards synergetic computers. In H. Haken (Ed.), *Complex systems—operational approaches* (pp. 225–240). Berlin: Springer-Verlag.

Singer, W., & Gray, C. M. (1995). Visual feature integration and the temporal correlation hypothesis. *Annu. Rev. Neurosci., 18*, 555–586.

Softky, W. (1994). Submillisecond coincidence detection in active dendritic trees. *Neuroscience, 58*, 13–41.

Somers, D. C., Nelson, S. B., & Sur, M. (1995). Analysis of temporal dynamics of orientation selectivity in feedback and feedforward models of visual cortex. *J. Neurosci., 15*, 5448–5465.

Spruston, N., Jaffe, D. B., Williams, S. H., & Johnston, D. (1993). Voltage- and space-clamp errors associated with the measurement of electrotonically remote synaptic events. *J. Neurophysiol., 70*, 781–802.

Steriade, M., Dossi, R. C., Pare, D., & Oakson, G. (1991). Fast oscillations (20–40Hz) in thalamocortical systems and their potentiation by mesopontine cholinergic nuclei in the cat. *Proc. Natl. Acad. Sci. USA, 88*, 4396–4400.

Thomson, A. M., & Deuchars, J. (1994). Temporal and spatial properties of local circuits in neocortex. *Trends Neurosci., 17*, 119–126.

Tsai, K. Y., Carnevale, N. T., Claiborne, B. J., & Brown, T. H. (1994). Efficient mapping from neuroanatomical to electrotonic space. *Network, 5*, 21–46.

Verschure, P. F. M. J. (1997). *Xmorph: A software tool for the synthesis and analysis of neural systems* (Tech. Rep.). Zurich: Institute of Neuroinformatics, ETH-UZ.

Verschure, P. F. M. J. (1998). Synthetic epistemology: The acquisition, retention, and expression of knowledge in natural and synthetic systems. In *Proceedings of IEEE World Conference on Computational Intelligence* (Anchorage), 147–153.

von der Malsburg, C. (1981). *The correlation theory of brain function* (Internal Rep. No. 81-2, 1–39). Max-Planck-Institute for Biophysical Chemistry.

von der Malsburg, C. (1995). Binding in models of perception and brain function. *Curr. Opinion Neurobiol., 5*, 520–526.

Wang, Z., & McCormick, D. A. (1993). Control of firing mode of corticotectal and corticopontine layer 5 burst-generating neurons by norepinephrine, acetylcholine, and 1 S,3R-ACPD. *J. Neurosci., 13*, 2199–2216.

Wilson, C. J. (1995). Dynamic modification of dendritic cable properties and synaptic transmission by voltage-gated potassium channels. *J. Comput. Neurosc., 2*, 91–115.

Yuste, R., & Tank, D. W. (1996). Dendritic integration in mammalian neurons, a century after Cajal. *Neuron, 16*, 701–716.

Zador, A., Agmon-Snir, H., & Segev, I. (1995). The morphoelectrotonic transform: A graphical approach to dendritic function. *J. Neurosci., 15*, 1669–1682.